HHS Public Access

Author manuscript

Vet Ophthalmol. Author manuscript; available in PMC 2023 May 01.

Published in final edited form as:

Vet Ophthalmol. 2022 May ; 25(Suppl 1): 84–95. doi:10.1111/vop.12943.

Development and validation of methods to visualize conventional aqueous outflow pathways in canine primary angle closure glaucoma

Mary Rebecca Telle, DVM[1,†], **Kevin C. Snyder, DVM, MS**[1,2], **Kazuya Oikawa, BVSc, PhD**[1,2], **Jacob P. Nilles, DVM**[1], **Shaile Gehrke, DVM**[1,2], **Leandro B.C. Teixeira, DVM, MS**[3], **Julie A. Kiland, MS**[2], **Alex Huang, MD, PhD**[4], **Gillian J. McLellan, BVMS, PhD**[1,2,*]

[1]Department of Surgical Sciences, School of Veterinary Medicine, University of Wisconsin-Madison, WI, USA

[2]Department of Ophthalmology & Visual Sciences, School of Medicine and Public Health, University of Wisconsin-Madison, WI, USA

[3]Department of Pathobiological Sciences, School of Veterinary Medicine, University of Wisconsin-Madison, WI, USA

[4]Shiley Eye Institute, The Viterbi Family Department of Ophthalmology, University of California, San Diego, CA, USA

Abstract

Purpose.—Angle closure glaucoma (PACG) is highly prevalent in dogs and is often refractory to medical therapy. We hypothesized that pathology affecting the post-trabecular conventional aqueous outflow pathway contributes to persistent intraocular pressure (IOP) elevation in dogs with PACG. The goal of this study was to determine the potential for aqueous angiography (AA) and optical coherence tomography (OCT) to identify abnormalities in post-trabecular aqueous outflow pathways in canine PACG.

Methods.—AA and anterior segment OCT (Spectralis HRA+OCT) were performed *ex vivo* in 19 enucleated canine eyes (10 normal eyes and 9 irreversibly blind eyes from canine patients enucleated for management of refractory PACG). Eyes were cannulated and maintained at physiologic IOP (10–20 mmHg) prior to intracameral infusion of fluorescent tracer. OCT scleral line scans were acquired in regions of high and low peri-limbal AA signal. Eyes were then perfusion fixed and cryo-sections prepared from 10/10 normal and 7/9 PACG eyes and immunolabeled for a vascular endothelial marker.

Results.—Normal canine eyes showed segmental, circumferential limbal AA signal, whereas PACG eyes showed minimal or no AA signal. AA signal correlated with scleral lumens on OCT in normal dogs, but lumens were generally absent or flattened in PACG eyes. Collapsed vascular

*Corresponding author: Gillian J. McLellan, Medical Sciences Center, 1300 University Avenue, Madison, WI 53706, +1-608-265-9848, gillian.mclellan@wisc.edu.

†Dr Telle's current address is: Department of Clinical Sciences, College of Veterinary Medicine, Mississippi State University, MS, USA

profiles were identified in tissue sections from PACG eyes, including those in which no lumens were identified on AA and OCT.

Conclusions.—In canine eyes with PACG, distal aqueous outflow channels are not identifiable by AA, despite normalization of their IOP, and intra-scleral vascular profiles are collapsed on OCT and histopathology.

Keywords

Aqueous angiography; glaucoma; dog; angle closure; OCT; distal aqueous outflow

Introduction

Primary angle closure glaucoma (PACG) is an important and prevalent cause of blindness and pain in dogs. In this species, PACG is often associated with pre-existing goniodysgenesis and dysplasia of the pectinate ligament which spans the iridocorneal angle opening. This abnormality is believed to have an underlying genetic basis especially in purebred dogs.[1–4] In humans, goniodysgenesis is an important cause of pediatric glaucoma. In dogs, however, acute collapse of the irido-ciliary cleft and iridocorneal angle (ICA) closure with an iris-like tissue commonly lead to acute, often extreme, IOP elevation in adulthood. The precise relationship between goniodysgenesis and subsequent development of glaucoma remains unclear, as only a relatively small proportion of dogs diagnosed with goniodysgenesis go on to develop PACG. . Although disruption of the conventional aqueous outflow pathways contributes to detrimental increases in IOP in both open angle and angle closure glaucomas, full understanding of the complex pathophysiology of aqueous humor outflow abnormalities in glaucoma remains elusive in both humans and dogs. In dogs, as in humans, conventional outflow of aqueous humor is through the corneoscleral trabecular meshwork (TM) and the angular aqueous plexus (analogous to the continuous canal of Schlemm in humans, and with similar physiology), with outflow continuing distally via collector channels and aqueous veins to a scleral venous plexus and to episcleral veins, respectively.[5–8]

Gonioscopy remains a primary diagnostic method in the evaluation of human and veterinary patients with glaucoma.[3, 9–10] Although gonioscopy is very commonly performed, the technique is used only to examine the anterior ICA and pectinate ligament that spans it in dogs, but does not necessarily allow for examination of deeper structures critical to aqueous humor outflow, such as trabecular meshwork within the ciliary cleft (CC),[11] and interpretation is relatively subjective and clinician dependent. Advanced imaging techniques such as high-resolution ultrasonography (HRUS) and ultrasound biomicroscopy (UBM) show promise in their ability to assess not only the ICA, but also more distal components of the conventional aqueous outflow pathway.[12–17] Optical coherence tomography (OCT) is another advanced cross-sectional imaging technique that can aid in the characterization of anterior segment morphology in patients with glaucoma and glaucoma suspects.[18–21] Still, these cross-sectional techniques are generally only practical for evaluation of very small sectors of the extensive, circumferential (360 degree) aqueous humor outflow pathways and they have relatively low sensitivity in detecting abnormalities of the trabecular portion of outflow pathways.[18–21] Further complicating the use of existing imaging techniques and

gonioscopy, aqueous humor outflow has been described as segmental in several models and species,[22–30] establishing that resistance to aqueous humor flow is likely not uniform circumferentially around the globe. Lastly, histopathology of enucleated globes can provide information regarding the cause of glaucoma,[31] but the ability to fully evaluate aqueous outflow pathways on histopathology is confounded by artifacts associated with prior surgical intervention, including enucleation surgery, fixation, embedding, and sectioning. We have observed, subjectively, that there appear to be fewer visible lumens in the sclera of canine eyes enucleated for PACG. However, without rigorous evaluation of multiple serial sections encompassing distal aqueous outflow pathways, histopathology is subject to the same limitations as other cross-sectional modalities as well as subjective, inter-observer variability.[32–34]

Previously published reports of advanced imaging techniques such as canalography and tracing of fluorescent microspheres have provided a solid framework for imaging outflow pathways *ex vivo* in the human[35] and porcine eye.[36, 37] Specifically, reports of aqueous angiography (AA), which allows circumferential and dynamic assessment of aqueous outflow, indicate that it can be effectively applied in feline, porcine, bovine, non-human primate, and human eyes *ex vivo*[24–29, 38] and in human patients *in vivo*.[29,39] This imaging technique enables the acquisition of real-time, qualitative and semi-quantitative information on circumferential and distal components of the conventional aqueous outflow system under physiologic IOP conditions.

Existing diagnostic techniques including gonioscopy and ocular ultrasonography have significant limitations and do not appear to be highly predictive of either glaucoma development or response to treatment, making early detection and diagnosis of this condition difficult in a veterinary clinical setting. There is a critical need for improved clinical methods to evaluate conventional aqueous humor outflow pathways to help guide treatment strategies and improve prognosis for PACG in canine and human patients alike. Our aims for this study were to develop and validate a non-invasive, clinically applicable tool for characterization of aqueous outflow in normal canine eyes and eyes of dogs with PACG, and to determine effects of PACG on the post-trabecular aqueous humor outflow pathways in dogs. Enhanced visualization and understanding of distal aqueous humor outflow pathways in at-risk patients may enable improved treatment planning, tailored to the individual patient. A recent study, published after the present study was completed, presents the use of intracameral injection of fluorescent tracer in normal canine eyes *in vivo*.[30] Here, we present findings of AA and OCT performed within a controlled range of IOP in normal and PACG-affected canine eyes, *ex vivo*, with histologic validation.

Methods

Test subjects:

Verbal and written informed consent were obtained from owners of eight dogs with PACG, allowing use of eyes from their dogs in this study immediately following enucleation for clinical reasons (Table 1). Normal canine eyes were obtained immediately postmortem from 10 female Beagle dogs that were euthanized for reasons not related to this study. These dogs ranged in age from 6 months to 2 years old. Blind eyes were enucleated for the management

of discomfort associated with glaucoma refractory to medical therapy in 7/9 eyes. In 2/9 glaucoma eyes, the owners elected enucleation of blind eyes for intermittent episodes of discomfort although the IOP was controlled medically at the time of enucleation in these animals. The animals in the PACG group ranged in sex, age, and breed (Table 1). All dogs included in the PACG group had at least one complete ophthalmic examination including gonioscopy performed by a board-certified veterinary ophthalmologist and were presumed to have PACG based on clinical signs and presentation, gonioscopic findings, and response or lack of response to treatment. There were 9 eyes total in the PACG group. One dog had both eyes enucleated due to PACG at different times during the 2-year course of the study, and both eyes were included in the study.

Aqueous angiography (AA):

Eyes were obtained following trans-palpebral enucleation with adnexa intact, immediately post-mortem in normal dogs and immediately post-enucleation in PACG dogs. As previously described for ex vivo human, porcine, feline, and bovine eyes,[24–26, 38] aqueous angiography was performed in eyes ex vivo within 24 hours of enucleation. Post-enucleation, eyes were wrapped in a phosphate-buffered saline (PBS) soaked gauze and kept in a sealed specimen cup at 4°C. Each globe was pinned to modeling clay after proper orientation was confirmed by the position of the nictating membrane and long posterior ciliary arteries and direction of the attached optic nerve. A 22g needle was used to make a perilimbal corneal paracentesis at either the 2 o'clock or 10 o'clock position for each eye, through which a 20g Lewicky anterior chamber maintainer was placed. Each eye was pre-perfused with balanced salt solution (BSS) (Alcon, Fort Worth, Texas) which was connected to a reservoir bag and maintained within normal physiologic range of IOP for dogs. The IOP was measured using rebound tonometry (Icare® TONOVET, Icare Oy, Finland) and was maintained at 10–20 mmHg for 30 minutes by adjusting the height of the BSS reservoir, as necessary. Typically, the reservoir height was approximately 25–30cm above the globe. BSS drops were applied topically to the cornea every 2–3 minutes to prevent corneal desiccation.

BSS was then exchanged for fluorescent tracer, either 2.5% fluorescein (Akorn, Illinois) or 0.4% indocyanine green (ICG) (Diagnostic Green, LLC, Farmington Hills, MI) in BSS that was infused into the anterior chamber at physiologic IOP. ICG was used first followed by fluorescein in 10/10 of the normal dog eyes, and in 4/9 of the PACG dog eyes. Because indocyanine green has a longer intraluminal presence and there were no appreciable differences between the tracers, the remaining 4 PACG eyes were imaged with ICG only.

Using an anterior segment module lens, aqueous angiography (AA) was performed using the Spectralis HRA+OCT (Heidelberg Engineering Inc., Carlsbad, CA). To provide background images and ensure adequate focus of the images, confocal scanning laser infrared images were taken prior to tracer introduction in the anterior chamber. Immediately upon exchange of BSS for tracer, AA images were acquired at 3–5 minute intervals around the limbus for each quadrant for up to 45 minutes post-infusion of tracer. Baseline sensitivity was set at 50. Quadrants with little to no apparent angiographic signal were termed "low signal", and quadrants with any signal present were termed "high signal". In all cases where signal was observed, the signal was seen in under 10 minutes. Exact times are not available given that

images were captured in 3–5 minute intervals for each quadrant. In those areas with no signal, the sensitivity was increased to confirm absence of signal.

One PACG eye (G8) had dense corneal and conjunctival pigment from chronic ocular surface disease that precluded evaluation of AA, and was thus excluded at this point in the experiment

Spectral domain optical coherence tomography (SD-OCT):

To determine whether angiographically positive regions correlated with lumens, scleral line scans were obtained in 10/10 normal eyes and 8/9 PACG eyes with the anterior segment module on sclera mode in both high and low flow areas simultaneously during AA using Spectralis HRA+OCT. Although the 15-degree scleral line scans were typically oriented perpendicular to the limbus, scan orientation was also modified in specific areas where perpendicular orientation proved challenging.

Immunofluorescent labeling:

Following angiography, each eye was perfusion fixed at physiologic IOP (10–20 mmHg) for 10 minutes with 4% paraformaldehyde in 0.1M PBS (PFA). The globes were then transferred to 0.1M PBS after immersion fixation overnight in 4% PFA at 4°Celsius. Based on AA signal, high signal and low signal sectors were identified for 10/10 normal and 7/9 PACG eyes. The pigmented globe (G8) was excluded, and one globe (G1.1) was lost after submission for histopathology and thus could not be further evaluated in the study. A thin sagittal section of the globe containing the pupil and the optic nerve was obtained and set aside for paraffin embedding and light microscopy. The remaining two calottes of the globe were hemisected at the equator and the portions of the anterior segment thereby dissected into quadrants circumferentially. A sector was dissected for each high- and low-flow quadrant (approximately 2mm wide extending 2 mm posterior to limbus) and was sucrose protected with 15% then 30% sucrose in 0.01M PBS at 4°C. Tissues were then cryo-embedded and longitudinally cryo-sectioned at 10μm by the Translational Research Initiatives in Pathology laboratory at UW-Madison. Cryosections were first incubated for 1 hour at room temperature in a permeabilization and a blocking step (10% normal donkey serum + 1% Bovine serum albumin + 0.1% Triton-X100 in 0.01M PBS). Sections were then incubated overnight at 4°C, with primary antibody for the vascular endothelial marker, von Willebrand Factor (vWF; Novus Biologicals, at 1:2000 dilution in 0.01M PBS). Alexa®Fluor 568 conjugated secondary antibody was used to detect bound primary antibody (1:400 dilution in 0.01M PBS) for 40 mins at RT, protected from light, and sections then washed with 0.01M PBS for 15 mins. Nuclei were counter-stained with DAPI (1:1,000 dilution in 0.01M PBS), and each slide was washed then mounted with an anti-fade aqueous mounting medium (ProLong® Gold, Invitrogen). Canine small intestine and kidney tissue cryosections from normal dogs were used as positive controls. For each IHC run omission of primary antibody from one section per target served as negative controls. Fluorescence photomicrographs were obtained at 5x-20x magnification (Axio Imager with Zen Pro software; Zeiss, Germany).

Histopathology:

For all normal and PACG eyes, the previously obtained thin sagittal section of the globes were routinely processed for light microscopy by paraffin embedding, and 5μm-thick microtome sections obtained were stained with Hematoxylin and Eosin (H&E). All sections were reviewed by a board-certified veterinary pathologist (LBCT), for histopathological confirmation of the diagnosis of PACG or to confirm absence of lesions (normal eyes).

Results

Aqueous angiography:

In all normal eyes, high quality aqueous angiography images were obtained circumferentially (Figure 1A). In 10/10 normal eyes, segmental regions of angiographic signal were noted (Figure 1B), with strong angiographic signal in some areas and weaker signal in others. The segmental outflow pattern was unique in each eye, and no single quadrant with apparent higher outflow was consistently identified. Overall, the outflow pattern was similar across all normal eyes with no subjective major differences in architecture of outflow channels. No objective quantitative measures were performed in this proof-of-concept study. The anterior chamber maintainer was placed in two different locations to investigate whether the location of the maintainer influenced the location of high- or low-flow AA signal, and no difference was noted, subjectively.

In 6/8 PACG eyes (Figures 2–4), no angiographic signal was appreciated despite some of these globes having small, collapsed intra-scleral lumens observed with OCT (see below). Two PACG eyes (G1.2 and G4) exhibited a small region of low-intensity fluorescence but this was not typical of the normal, branching distal outflow signal, and in each eye was confined to one quadrant. One PACG eye (G8) had dense corneal and conjunctival pigment from chronic ocular surface disease that precluded visualization of any AA fluorescent signal.

SD-OCT:

Scleral line scans obtained simultaneously during AA identified hypo-reflective lumens corresponding to angiographic signal in normal canine eyes (Figure 5). There were also lumens identified in areas of low angiographic signal in normal dogs with segmental outflow. Although the lumens appeared, subjectively, fewer in number in these regions, this observation was not objectively quantified. For the majority of quadrants scanned in PACG eyes, there were no lumens visible on SD-OCT. However, even in the absence of an angiographic signal lumens could occasionally be seen in some regions on SD-OCT in PACG dogs, with the exception of dog PACG eye G8, in which ocular surface hyperpigmentation precluded OCT imaging. However, these intra-scleral lumens appeared relatively sparse compared to normal eyes and were subjectively collapsed and abnormal in profile (Figure 6).

Immunofluorescence labeling:

Labeling for a vascular endothelial marker (vWF) confirmed that the intra-scleral hyporeflective lumens seen on SD-OCT in normal canine eyes were indeed vessels (Figure

7). Contrary to OCT findings, collapsed lumens were identifiable in “no flow” areas of PACG eyes, that were not visualized on AA or SD-OCT (Figure 8).

Histopathology:

All eyes in the PACG group were confirmed to have goniodysgenesis and posterior segment features consistent with end stage glaucoma. The diagnosis of goniodysgenesis was based on the presence of a poorly formed iridocorneal angle characterized by the replacement of the normal pectinate ligaments and ciliary cleft opening by an iris-like tissue that directly attaches to the arborizing end of Descemet’s membrane along with a complete to partial absence of an identifiable the ciliary cleft and trabecular meshwork tissue and paucity of the angular aqueous plexus structures (Figure 9). The glaucomatous changes in the retina and optic nerve included inner-to-full thickness retinal atrophy and varying degrees of optic nerve head gliosis, cupping and atrophy. Additionally, histopathology identified a preiridal fibrovascular membrane in 4/7 eyes and pigment dispersion in the trabecular meshwork in 5/7 eyes of the PACG group. These additional lesions were interpreted to be secondary with a minor contribution to the impairment of the aqueous outflow, and goniodysgenesis was identified as the primary cause of glaucoma in all eyes in the PACG group. Histologic sections of PACG eyes were also examined for the presence of intra-scleral vascular lumens. Intra-scleral lumens were very sparse in 2/7 or were not visualized in 5/7 H&E-stained sections of the eyes, even though immunofluorescent labeling confirmed their presence in similarly oriented cryosections.

Discussion

This is the first report of aqueous angiography in canine eyes with PACG *ex* vivo. This technique produced high quality circumferential AA images in normal canine eyes, and helped characterize outflow patterns, or lack thereof, in dogs with PACG.

In normal canine eyes, the dynamic AA signal suggested segmental outflow with no consistent pattern observed to indicate that the distribution of segmental high and low outflow signal differed by limbal region. These findings are similar to previous reports of segmental outflow using the same technique in enucleated canine,[30] porcine,[24] bovine,[26] feline,[38] and human eyes,[24] as well as live non-human primate[27] and human[28, 29, 39] eyes. In contrast, no robust AA signal was evident in any of the PACG eyes in this study. Scleral SD-OCT scans revealed hypo-reflective lumens corresponding to the angiographic signal in normal canine eyes. It is noteworthy that SD-OCT also revealed occasional visible lumens in some of the PACG eyes that had no visible angiographic signal on AA. To further evaluate the presence or absence of scleral lumens, immunofluorescent labeling was performed in both normal and PACG eyes. This technique allowed visualization of collapsed intrascleral vascular profiles in both groups, even in areas with no AA signal that had no visible lumens on SD-OCT. Subjectively, the lumens in PACG eyes were small and mostly collapsed, whereas the lumens in normal eyes were more robust in size and number. These findings indicate that even severely affected PACG eyes *do* have scleral lumens but might suggest that some combination of vascular lumen abnormalities in distal outflow pathways (e.g.

structure, function, perfusion, lumen size, collapsibility) could be contributing to reduction in aqueous outflow in PACG-affected eyes.

There are visible differences in the architecture of scleral lumens in normal dogs versus PACG dogs, and it is possible that animals with PACG are born with normal scleral lumens, but collapse of these channels subsequently occurs, as visualized on SD-OCT and immunofluorescent labeling. Whether a cause or effect of IOP elevation, this collapse of distal outflow channels may further compound aqueous humor outflow obstruction. However, because all of the eyes in the PACG group were from adult dogs with established glaucoma, assumptions cannot be made about the morphology of these eyes earlier in life. Abnormal scleral lumens may conceivably have been a congenital feature which predisposed these eyes to PACG. Alternatively, and more likely, collapse of distal aqueous outflow vessels could also have been an acquired feature, whether primary or secondary. Further investigations will be necessary to elucidate the nature of the relationship between distal outflow vessels, resistance to aqueous outflow, IOP and glaucoma. It is noteworthy that two eyes in the study had IOP that had normalized following medical therapy before enucleation and these eyes exhibited a very limited angiographic signal on AA and had some abnormal and collapsed scleral lumens with immunofluorescent labeling. This could indicate a dynamic process beginning with high IOP causing collapse of vessels, and after the IOP is normalized with topical glaucoma medications, distal outflow pathways are re-established, at least in some eyes, allowing for partial reappearance of AA signal. It must also be considered, however, that lack of perfusion via more proximal outflow structures, e.g. via complete obstruction of the opening of the ciliary cleft and the trabecular meshwork, may be a contributor to outflow impediment. Notably, iris-like tissue spanning the iridocorneal angle was a common histopathologic feature in eyes with PACG and likely the major contributor to outflow obstruction. These structures were not directly evaluated in *vivo* prior to IOP elevation or during IOP elevation, nor were they directly evaluated during *ex vivo* imaging in these patients. One exception to this was the second eye of dog G1, which exhibited pectinate ligament dysplasia in eye G1.2 at the time of initial presentation for glaucoma in eye G1.1. These proximal outflow structures were, however, evaluated using histopathology in this study, albeit in a very limited section of these circumferential structures.

A number of important limitations of this study must be considered. Most importantly, this study was performed *ex vivo*, and therefore the results presented here may not be replicated *in vivo*. Notably, a recent report of AA in normal canine eyes *in vivo*, published after the current study was completed, presented inconsistent results *in vivo* using the cannulation method we used in the current study, but was able to acquire similar delineation of the distal outflow pathway by direct intracameral injection of fluorescent tracer in normal living canine eyes.[30] In contrast to that prior report,[30] in which IOP was not maintained in a consistent range during imaging which limited ability to draw comparisons between eyes and sessions, care was taken in the current study to maintain consistent IOP during imaging by perfusion of BSS or tracer using gravity assisted perfusion from a reservoir. However, this cannot be considered maintenance of true physiological IOP conditions, as there is no venous pressure component in this *ex vivo* model, and this likely impacts both proximal and distal structures involved in aqueous outflow, including scleral lumens. Other limitations of this proof-of-concept pilot study include small sample size with lack of sex-

and age-matched controls, as normal dogs were all female and were younger than dogs in the glaucoma group.

Importantly, we demonstrated that observation of lack of intrascleral lumens on SD-OCT images and in conventional histopathology sections must be interpreted very carefully. Standard SD- OCT is not able to detect characteristic hypo-reflective signals from the lumens of vessels that are collapsed. No attempt was made to quantify angiographic signal or measure lumen dimensions in this study. For quantitative studies it will be important to obtain scleral line scans with perfect orientation perpendicular to the limbus, or perpendicular to specific vessels, in order to obtain the most consistent information, and this orientation was not achieved in many of the enucleated globes in this study, in part due to the learning curve for scan acquisition. Nevertheless, our observation that scleral vessels are collapsed, corresponding to complete lack of angiographic signal in dogs with PACG refractory to medical therapy despite normalization of IOP, could suggest a potential novel prognostic indicator in dogs with PACG, if it were shown in vivo that absence of visible scleral lumens following acute IOP lowering correlated with poorer long-term response to medical or surgical therapies that rely solely on reduction of aqueous production or on enhancement of conventional outflow.

In conclusion, this is the first report of AA in canine eyes with PACG. Most PACG eyes showed little evidence of distal outflow on AA despite normalization of their IOP, and vascular profiles were absent to collapsed on OCT and histopathology. This study shows that AA is a valid technique to image distal aqueous humor outflow pathways in the canine eye *ex vivo*, especially when assessing 360 degrees around the globe. Thus, our findings may have direct, practical, translational relevance in the assessment of canine glaucoma patients and suspects in a clinic setting. However, further, longitudinal studies are needed *in vivo*, together with studies to determine the effect of IOP elevation on AA signal and scleral lumen profiles, in both normal dogs and dogs with PACG, in order to more definitively establish the relevance of these findings to the pathophysiology of PACG in dogs.

Acknowledgments

Supported by ACVO Vision for Animals Foundation; Unrestricted Funds to the University of Wisconsin-Madison Department of Ophthalmology and Visual Sciences from Research to Prevent Blindness; NIH Grants P30 EY016665 and S10 OD018221 and T35OD011078

Financial disclosure: Heidelberg Engineering (Research Support, ASH), Glaukos Corporation (Research Support, ASH), Aerie Pharmaceuticals (Consultant, ASH), Diagnosys (Research Support, ASH).

This work was supported in part by funding from the National Institutes of Health (NIH).

References

1. Gelatt KN, MacKay EO. Prevalence of the breed-related glaucomas in pure-bred dogs in North America. Vet Ophthalmol. 2004 Mar-Apr 2004;7(2):97–111. doi:10.1111/j.1463-5224.2004.04006.x [PubMed: 14982589]
2. Komáromy AM, Petersen-Jones SM. Genetics of Canine Primary Glaucomas. Vet Clin North Am Small Anim Pract. Nov 2015;45(6):1159–82, v. doi:10.1016/j.cvsm.2015.06.003 [PubMed: 26277300]

3. Bedford PG. A gonioscopic study of the iridocorneal angle in the English and American breeds of Cocker Spaniel and the Basset Hound. J Small Anim Pract. Oct 1977;18(10):631–42. [PubMed: 604666]
4. Pugh CA, Farrell LL, Carlisle AJ, et al. Arginine to Glutamine Variant in Olfactomedin Like 3 (G3 (Bethesda) 03 2019;9(3):943–954. doi:10.1534/g3.118.200944 [PubMed: 30696701]
5. Cruise LJ, McClure R. Posterior pathway for aqueous humor drainage in the dog. Am J Vet Res. Jun 1981;42(6):992–5. [PubMed: 7283249]
6. Van Buskirk EM. The canine eye: the vessels of aqueous drainage. Invest Ophthalmol Vis Sci. Mar 1979;18(3):223–30. [PubMed: 422328]
7. Tripathi RC, Tripathi BJ. The mechanism of aqueous outflow in lower mammals. Exp Eye Res. Jul 1972;14(1):73–9. [PubMed: 4339120]
8. Tripathi RC. Ultrastructure of the exit pathway of the aqueous in lower mammals. (A preliminary report on the “angular aqueous plexus”). Exp Eye Res. Nov 1971;12(3):311–4. [PubMed: 5130275]
9. Bedford PG. Gonioscopy in the dog. J Small Anim Pract. Oct 1977;18(10):615–29. [PubMed: 604665]
10. Prum BE, Rosenberg LF, Gedde SJ, et al. Primary Open-Angle Glaucoma Preferred Practice Pattern(®) Guidelines. Ophthalmology. Jan 2016;123(1):P41–P111. doi:10.1016/j.ophtha.2015.10.053 [PubMed: 26581556]
11. Gibson TE, Roberts SM, Severin GA, Steyn PF, Wrigley RH. Comparison of gonioscopy and ultrasound biomicroscopy for evaluating the iridocorneal angle in dogs. J Am Vet Med Assoc. Sep 1998;213(5):635–8. [PubMed: 9731256]
12. Dubin AJ, Bentley E, Buhr KA, Miller PE. Evaluation of potential risk factors for development of primary angle-closure glaucoma in Bouvier des Flandres. JAVMA. 2017;250(1)
13. Marchini G, Pagliarusco A, Toscano A, Tosi R, Brunelli C, Bonomi L. Ultrasound biomicroscopic and conventional ultrasonographic study of ocular dimensions in primary angle-closure glaucoma. Ophthalmology. Nov 1998;105(11):2091–8. doi:10.1016/S0161-6420(98)91132-0 [PubMed: 9818611]
14. Tello C, Tran HV, Liebmann J, Ritch R. Angle closure: classification, concepts, and the role of ultrasound biomicroscopy in diagnosis and treatment. Semin Ophthalmol. Jun 2002;17(2):69–78. doi:10.1076/soph.17.2.69.14722 [PubMed: 15513459]
15. Bentley E, Miller PE, Diehl KA. Use of high-resolution ultrasound as a diagnostic tool in veterinary ophthalmology. J Am Vet Med Assoc. Dec 2003;223(11):1617–22, 1599. [PubMed: 14664449]
16. Hasegawa T, Kawata M, Ota M. Ultrasound biomicroscopic findings of the iridocorneal angle in live healthy and glaucomatous dogs. J Vet Med Sci. Jan 2016;77(12):1625–31. doi:10.1292/jvms.15-0311 [PubMed: 26212256]
17. Radhakrishnan S, Goldsmith J, Huang D, et al. Comparison of optical coherence tomography and ultrasound biomicroscopy for detection of narrow anterior chamber angles. Arch Ophthalmol. Aug 2005;123(8):1053–9. doi:10.1001/archopht.123.8.1053 [PubMed: 16087837]
18. Leung CK, Chan WM, Ko CY, et al. Visualization of anterior chamber angle dynamics using optical coherence tomography. Ophthalmology. Jun 2005;112(6):980–4. doi:10.1016/j.ophtha.2005.01.022 [PubMed: 15936438]
19. Almazan A, Tsai S, Miller PE, et al. Iridocorneal angle measurements in mammalian species: normative data by optical coherence tomography. Vet Ophthalmol. Mar 2013;16(2):163–6. doi:10.1111/j.1463-5224.2012.01030.x [PubMed: 22612298]
20. McLellan GJ, Rasmussen CA. Optical coherence tomography for the evaluation of retinal and optic nerve morphology in animal subjects: practical considerations. Vet Ophthalmol. Sep 2012;15 Suppl 2:13–28. doi:10.1111/j.1463-5224.2012.01045.x [PubMed: 22805095]
21. Bradfield Y, Barbosa T, Blodi B, et al. Comparative Intraoperative Anterior Segment OCT Findings in Pediatric Patients with and without Glaucoma. Ophthalmol Glaucoma. 2019 Jul - Aug 2019;2(4):232–239. doi:10.1016/j.ogla.2019.04.006 [PubMed: 32672544]
22. Swaminathan SS, Oh DJ, Kang MH, Rhee DJ. Aqueous outflow: segmental and distal flow. J Cataract Refract Surg. Aug 2014;40(8):1263–72. doi:10.1016/j.jcrs.2014.06.020 [PubMed: 25088623]

23. Johnson DH, Johnson M. Glaucoma surgery and aqueous outflow: how does nonpenetrating glaucoma surgery work? Arch Ophthalmol. Jan 2002;120(1):67–70. [PubMed: 11786060]
24. Saraswathy S, Tan JC, Yu F, et al. Aqueous Angiography: Real-Time and Physiologic Aqueous Humor Outflow Imaging. PLoS One. 2016;11(1):e0147176. doi:10.1371/journal.pone.0147176 [PubMed: 26807586]
25. Huang AS, Saraswathy S, Dastiridou A, et al. Aqueous Angiography-Mediated Guidance of Trabecular Bypass Improves Angiographic Outflow in Human Enucleated Eyes. Invest Ophthalmol Vis Sci. Sep 2016;57(11):4558–65. doi:10.1167/iovs.16-19644 [PubMed: 27588614]
26. Huang AS, Saraswathy S, Dastiridou A, et al. Aqueous Angiography with Fluorescein and Indocyanine Green in Bovine Eyes. Transl Vis Sci Technol. Nov 2016;5(6):5. doi:10.1167/tvst.5.6.5
27. Huang AS, Li M, Yang D, Wang H, Wang N, Weinreb RN. Aqueous Angiography in Living Nonhuman Primates Shows Segmental, Pulsatile, and Dynamic Angiographic Aqueous Humor Outflow. Ophthalmology. 06 2017;124(6):793–803. doi:10.1016/j.ophtha.2017.01.030 [PubMed: 28237425]
28. Huang AS, Camp A, Xu BY, Penteado RC, Weinreb RN. Aqueous Angiography: Aqueous Humor Outflow Imaging in Live Human Subjects. Ophthalmology. 08 2017;124(8):1249–1251. doi:10.1016/j.ophtha.2017.03.058 [PubMed: 28461013]
29. Huang AS, Penteado RC, Saha SK, et al. Fluorescein Aqueous Angiography in Live Normal Human Eyes. J Glaucoma. Nov 2018;27(11):957–964. doi:10.1097/IJG.0000000000001042 [PubMed: 30095604]
30. Burn JB, Huang AS, Weber AJ, Komáromy AM, Pirie CG. Aqueous Angiography in Normal Canine Eyes. Transl Vis Sci Technol. Aug 2020;9(9):44. doi:10.1167/tvst.9.9.44
31. Reilly CM, Morris R, Dubielzig RR. Canine goniodysgenesis-related glaucoma: a morphologic review of 100 cases looking at inflammation and pigment dispersion. Vet Ophthalmol. 2005 Jul-Aug 2005;8(4):253–8. doi:10.1111/j.1463-5224.2005.00399.x [PubMed: 16008705]
32. van der Linde-Sipman JS. Dysplasia of the pectinate ligament and primary glaucoma in the Bouvier des Flandres dog. Vet Pathol. May 1987;24(3):201–6. [PubMed: 3603960]
33. Smith R, Peiffer R, Wilcock B. Some aspects of the pathology of canine glaucoma. VETERINARY CLINICAL PATHOLOGY. 1993;22:16–16.
34. Bauer BS, Sandmeyer LS, Philibert H, Feng CX, Grahn BH. Chronic Glaucoma in Dogs: Relationships Between Histologic Lesions and the Gonioscopic Diagnosis of Pectinate Ligament Dysplasia. Vet Pathol. Nov 2016;53(6):1197–1203. doi:10.1177/0300985816642276 [PubMed: 27084398]
35. Cha ED, Xu J, Gong L, Gong H. Variations in active outflow along the trabecular outflow pathway. Exp Eye Res. 05 2016;146:354–60. doi:10.1016/j.exer.2016.01.008 [PubMed: 26775054]
36. Loewen RT, Brown EN, Scott G, Parikh H, Schuman JS, Loewen NA. Quantification of Focal Outflow Enhancement Using Differential Canalograms. Invest Ophthalmol Vis Sci. 05 2016;57(6):2831–8. doi:10.1167/iovs.16-19541 [PubMed: 27227352]
37. Loewen RT, Brown EN, Roy P, Schuman JS, Sigal IA, Loewen NA. Regionally Discrete Aqueous Humor Outflow Quantification Using Fluorescein Canalograms. PLoS One. 2016;11(3):e0151754. doi:10.1371/journal.pone.0151754 [PubMed: 26998833]
38. Snyder KC, Oikawa K, Williams J, et al. Imaging Distal Aqueous Outflow Pathways in a Spontaneous Model of Congenital Glaucoma. Transl Vis Sci Technol. Sep 2019;8(5):22. doi:10.1167/tvst.8.5.22
39. Huang AS, Penteado RC, Papoyan V, Voskanyan L, Weinreb RN. Aqueous Angiographic Outflow Improvement after Trabecular Microbypass in Glaucoma Patients. Ophthalmol Glaucoma. 2019 Jan-Feb 2019;2(1):11–21. doi:10.1016/j.ogla.2018.11.010 [PubMed: 31595267]

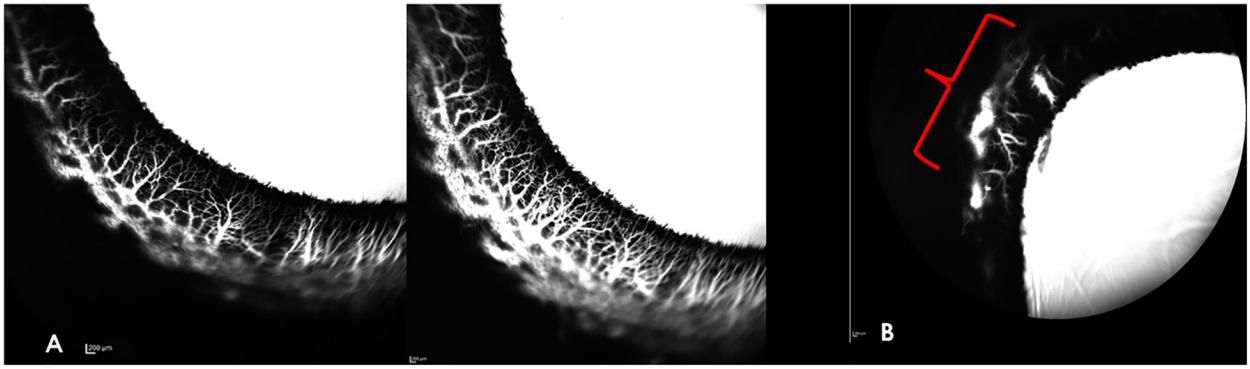

Figure 1.

Aqueous Angiography (AA) images of representative normal canine eyes obtained with indocyanine green (ICG). **A)** Representative high signal area in the temporal quadrant of the right eye. There is strong angiographic signal in the circumferential scleral vessels, depicted in white. The angiographic signal increased over time, with increase in intensity, density and complex branching of the smaller peri-limbal vessels perpendicular to the limbus as depicted in an image acquired 8.5 min post-tracer infusion (right panel) relative to the same region 2 minutes prior (left panel). **B)** Nasal quadrant of left eye (OS), illustrating segmental nature of AA signal. In this quadrant imaged 7 min after tracer infusion, there is an absence of angiographic signal, with the exception of only one relatively small region (indicated by red bracket) of low intensity, late onset, fluorescent signal.

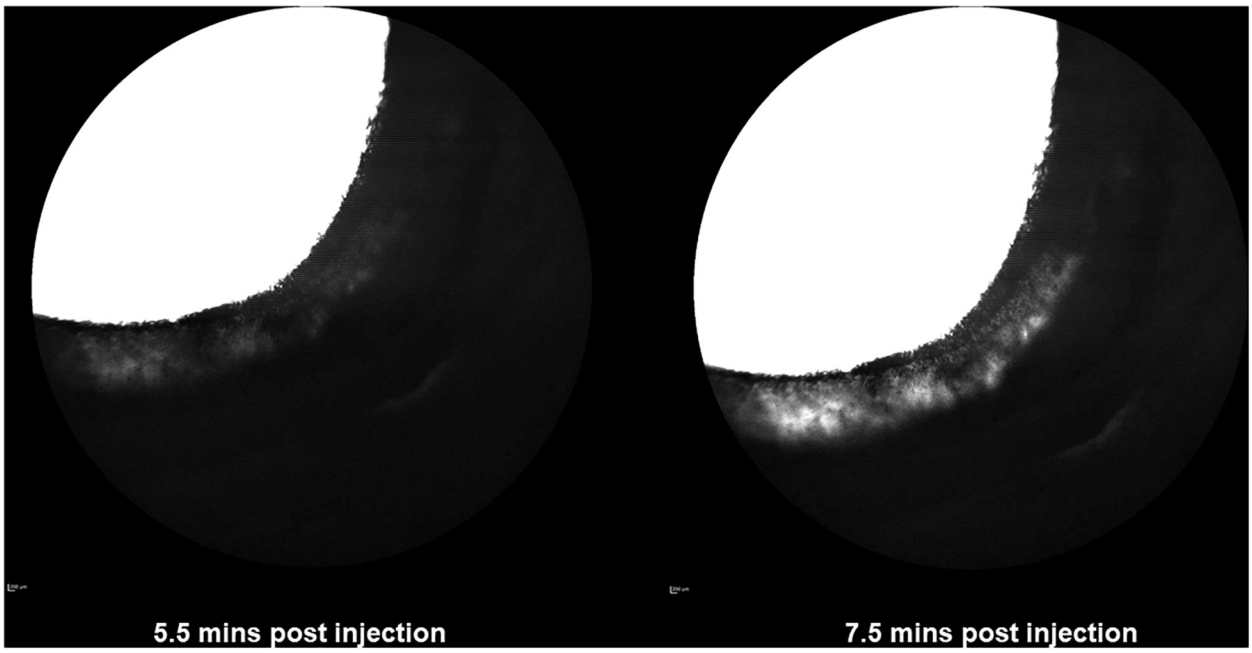

Figure 2.

Aqueous Angiography (AA) images of nasal quadrant of right eye (OD) (obtained with fluorescein for glaucomatous canine eye G1.1). There are no areas of well-defined AA signal. The “white” perilimbal areas appearing in the image on the right after more prolonged tracer infusion and increase in sensitivity setting, represent diffusion within scleral tissue and are not considered a true, intra-luminal, angiographic signal.

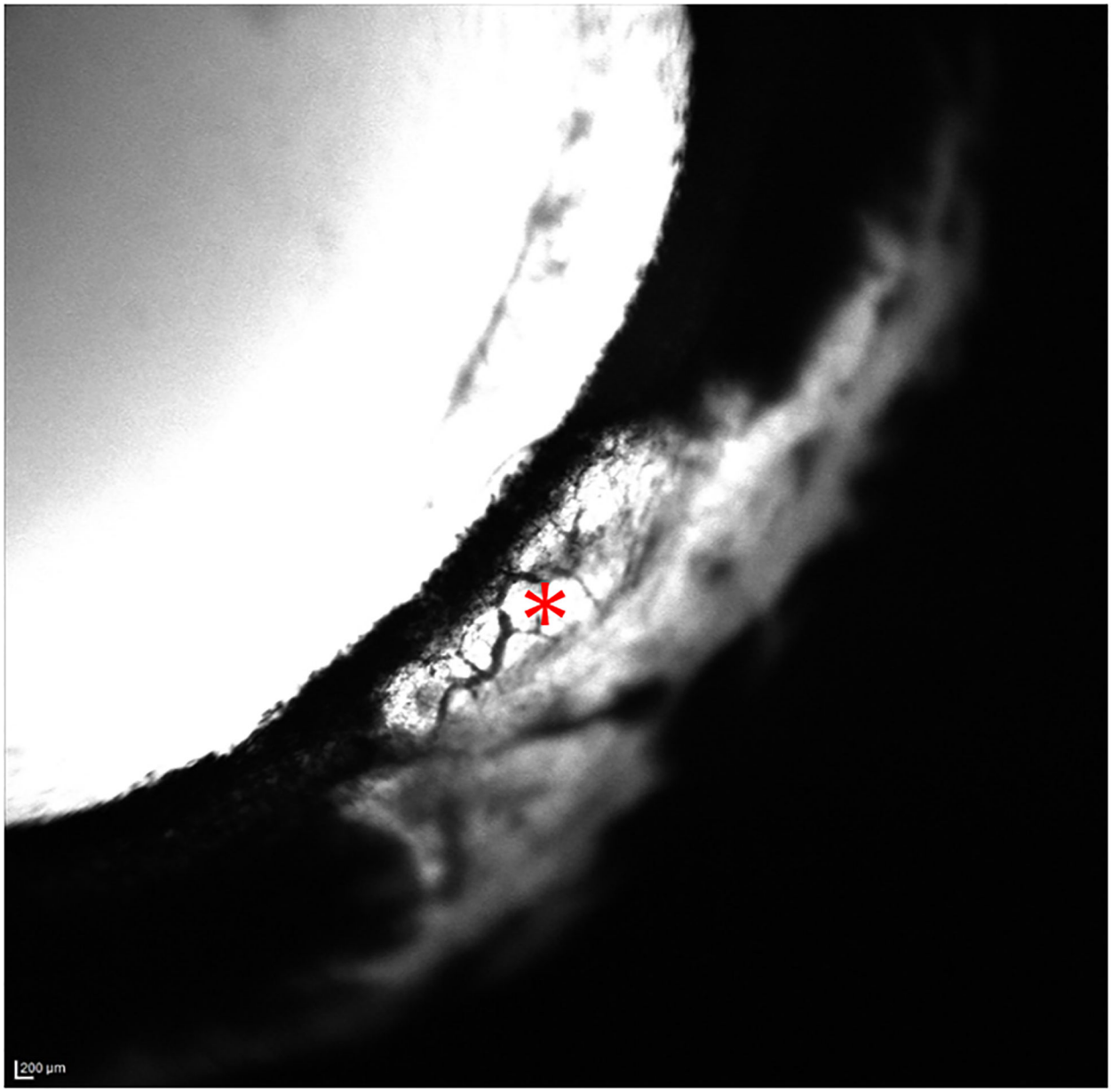

Figure 3.

Aqueous Angiography (AA) images of the temporal quadrant of the left eye (OS) acquired with indocyanine green (ICG) for glaucomatous eye G2. There are no areas of well-defined angiographic signal several minutes post-infusion of ICG. The white area of sclera appeared to represent fluorescence of dye in aqueous humor that was visible through thin sclera in this region, small perilimbal vessels that do not contain fluorescent tracer are visualized in these images as dark, branching structures against a fluorescent background (*), even when sensitivity settings were increased.

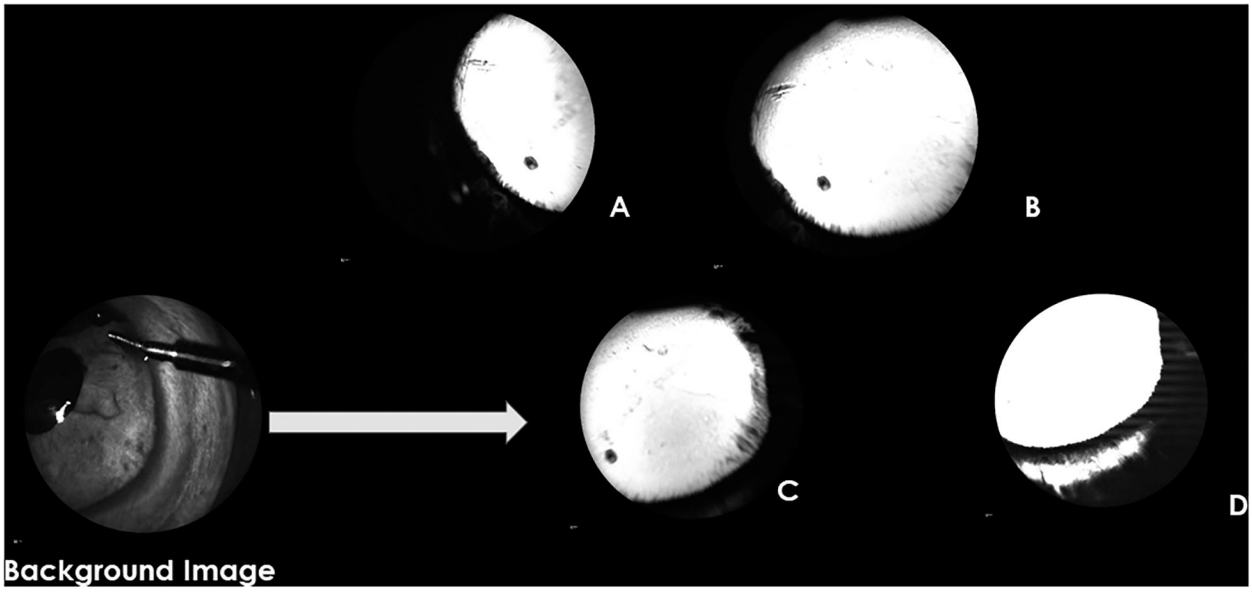

Figure 4.

Aqueous Angiography (AA) images obtained glaucomatous eye G4 following infusion of fluorescein. The background image shows the orientation of the right eye with the anterior chamber maintainer in the dorsonasal quadrant. A-D show images of different quadrants acquired around the 10-minute time point following tracer infusion (A=temporal, B=nasal, C=nasal, D=ventral). There are no areas of well-defined AA signal in any quadrant. The "white", hyperfluorescent area in D reflects scleral diffusion of fluorescein but is not considered representative of an AA signal.

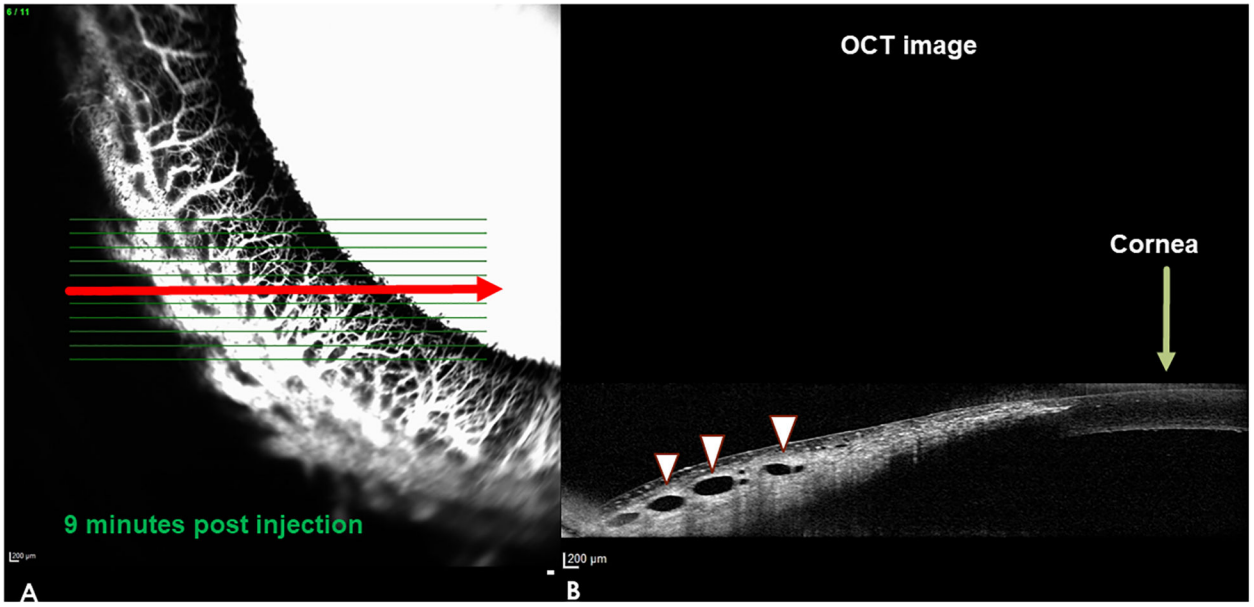

Figure 5.

Aqueous angiography (AA) and corresponding spectral domain optical coherence tomography (SD-OCT) images: representative normal dog eye, high signal area in the nasal quadrant of a left eye. The OCT image in **B)** corresponds with the line scan depicted by the red horizontal arrow on the AA image in **A)**. The OCT r line scan on the right resembles a histologic section through this region. The AA signal in **A)** corresponds to the dark, hyporeflective lumens seen on OCT (white arrow heads) **B).** Note that there is no AA fluorescent signal visible in the lumens (white arrow heads) on the OCT scan on the right because the laser wavelength used to acquire the angiographic signal is not imaged in this part of the scan.

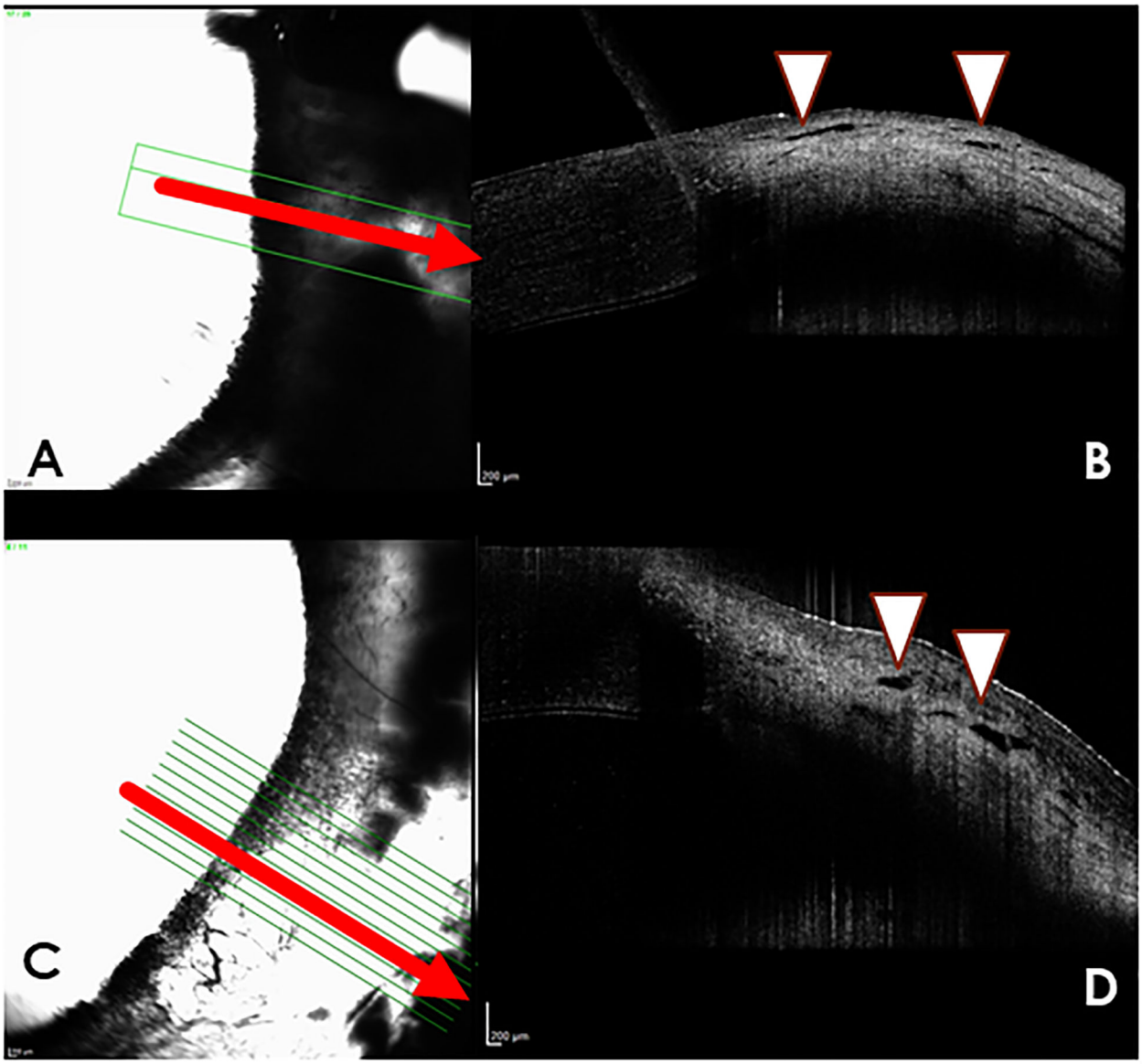

Figure 6.

Aqueous angiography (AA) with indocyanine green (A,C) and Spectral-domain optical coherence tomography (SD-OCT) images (B,D) from dogs with glaucoma. (A) Nasal quadrant of right eye of glaucomatous dog G4, “no flow” area with indocyanine green (ICG). There is minimal AA signal in this region. The corresponding OCT image (B) demonstrates very small, nearly collapsed scleral lumens (white arrow heads). (C) Temporal quadrant of left eye of glaucomatous dog G2, illustrates a “no flow” area with only diffuse fluorescence but no apparent intraluminal AA signal. (D) the corresponding OCT image demonstrates very small, nearly collapsed scleral lumens (white arrows) when compared to the normal dog.

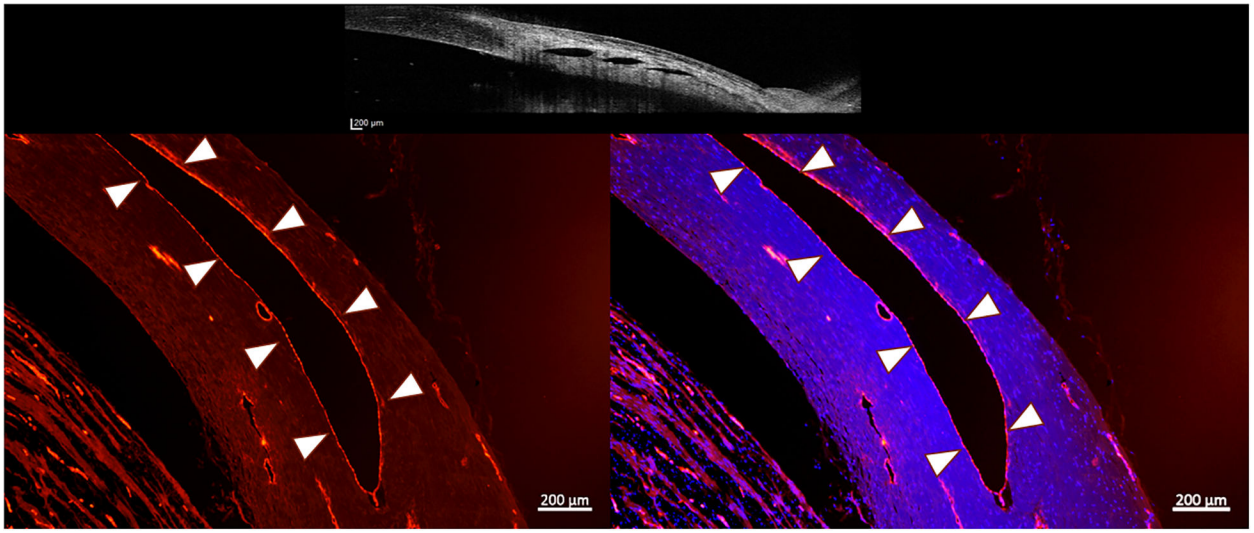

Figure 7.

Fluorescence photomicrographs of perilimbal sclera from a representative normal canine eye. The red immunofluorescent labeling by von Willebrand factor of vascular endothelium on the inner surface of each lumen (outlined by white arrow heads) confirms the vascular nature of these lumens (positive control). Right image, merged with blue fluorescent DAPI-stained nuclei (lumen highlighted with white arrow heads). Top image is an OCT image showing the scleral lumens being identified with positive controls. (Images intentionally overexposed to facilitate visualization of tissue morphology). (Bar Markers 200µm, 5X magnification)

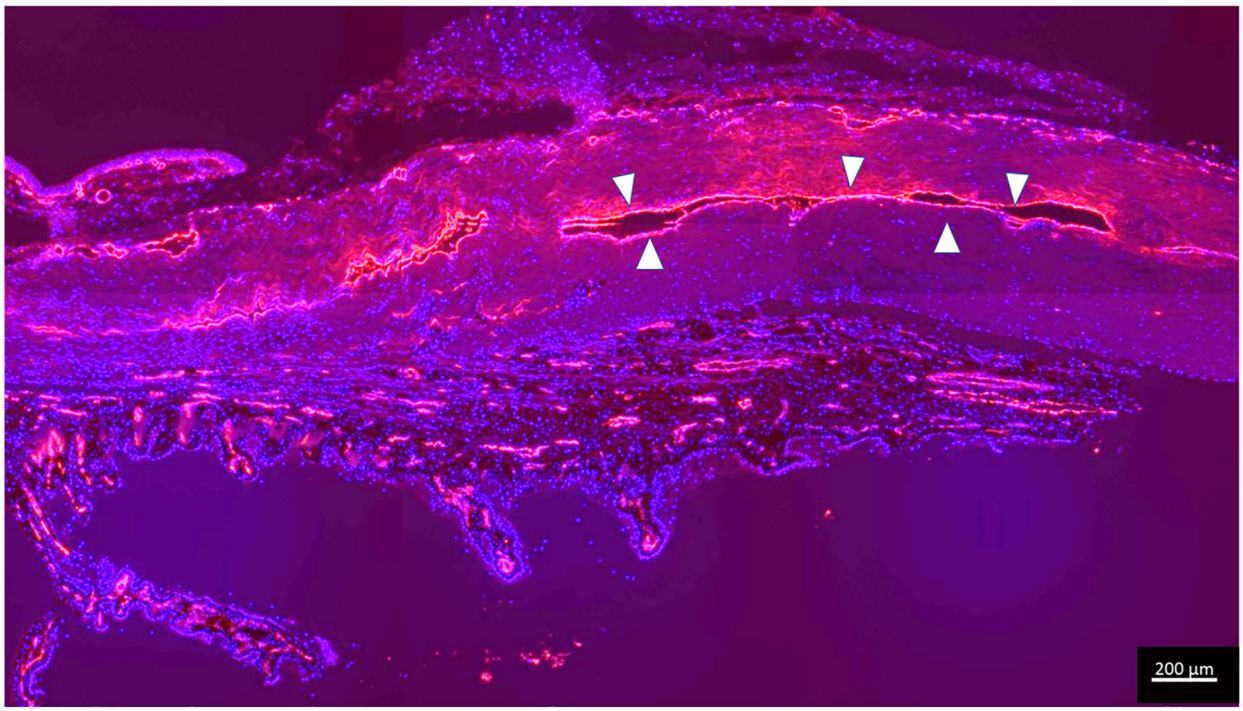

Figure 8.

Immunolabeling for endothelial marker confirms presence of collapsed scleral vessels in glaucomatous dog G2 which had no angiographic signal. Endothelial cells are highlighted in red (outlined in white arrow heads), lining the collapsed lumens with DAPI (blue nuclear counterstain). (Bar marker 200µm)

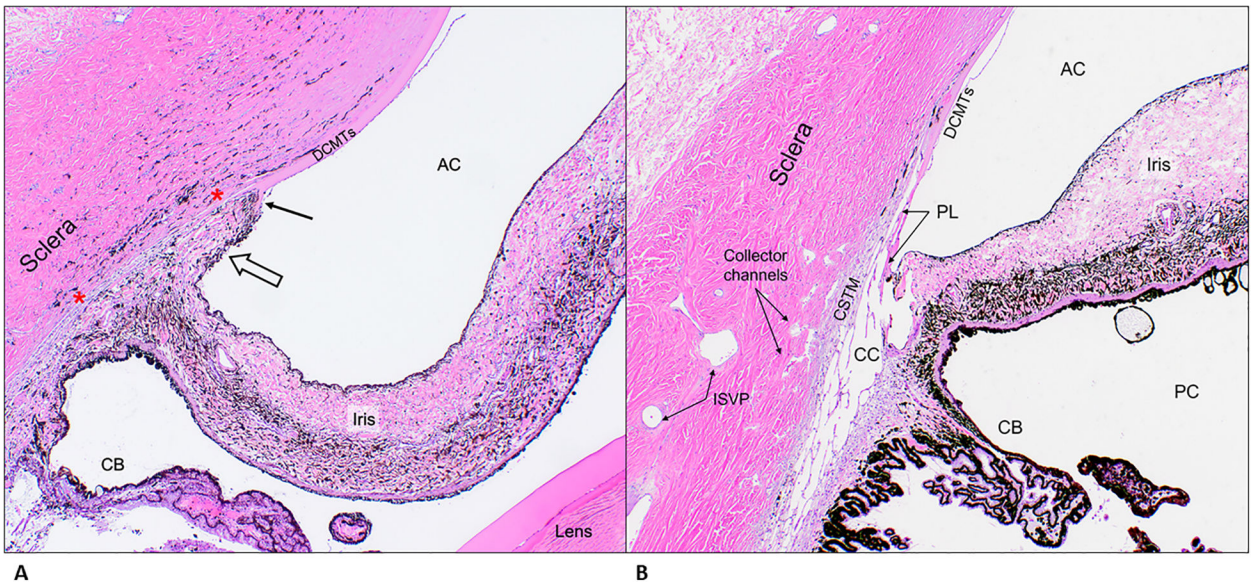

Figure 9.

A. Representative photomicrograph of a section of the iridocorneal angle from patient G5, a Leonberger, illustrating features consistent with primary glaucoma. Note an iris-like tissue (open arrow) crossing over the iridocorneal angle opening contacting the arborizing (fibrillating) end of Descemet's membrane (black arrow) replacing the normal pectinate ligaments and ciliary cleft opening. Also, in the region between the red asterixis, note the absence of an identifiable ciliary cleft and trabecular meshwork tissue and paucity of angular aqueous plexus structures. H&E, 4X objective. **B. Representative photomicrograph of** a section of the iridocorneal angle from a control dog illustrating the normal anatomical features. H&E, 4X objective. **AC**= anterior chamber; **DCMTs**= Descemet's membrane; **PL**= pectinate ligaments; **CSTM**= corneo-scleral trabecular meshwork; **CC**= ciliary cleft; **CB**= ciliary body; **PC**= posterior chamber; **ISVP**= intra-scleral venous plexus

Table 1.

Details of canine patients with primary angle closure glaucoma, including age, sex, breed, eye(s), duration of glaucoma, and status of IOP at time of enucleation. Whether aqueous angiography (AA), Optical Coherence Tomography imaging (SD-OCT), or immunofluorescent labeling of tissue sections was possible is also listed.

Dog	Age &Sex	Breed	Eye(s)	Duration of owner-observed clinical signs consistent with glaucoma upon initial presentation	IOP status at time of enucleation	AA	SD-OCT	Immunofluorescent labeling
G1.1	13 yo MC	Beagle Mix	OD	<48 hrs	Uncontrolled	Yes	Yes	No
G1.2	13 yo MC	Beagle Mix	OS	<48 hrs	Uncontrolled	Yes	Yes	Yes
G2	8 yo FS	American Cocker Spaniel	OS	<48 hrs	Uncontrolled	Yes	Yes	Yes
G3	10 yo FS	Siberian Husky	OD	Unknown	Uncontrolled	Yes	Yes	Yes
G4	12 yo MC	Lhasa Apso Mix	OD	Unknown	Uncontrolled	Yes	Yes	Yes
G5	6 yo MC	Leonberger	OD	~1 week	Controlled	Yes	Yes	Yes
G6	9 yo FS	Shih Tzu	OS	Unknown	Controlled	Yes	Yes	Yes
G7	10 yo MC	Labrador Retriever	OS	~1 week	Uncontrolled	Yes	Yes	Yes
G8	11 yo FS	Cockapoo	OD	Unknown	Uncontrolled	Not possible (pigment)	No (pigment)	No

MC = male, castrated; FS = female, spayed; OD = right eye; OS = left eye; controlled IOP = ≤ 25 mmHg; uncontrolled IOP = > 25 mmHg